Supporting Information

Toy et al. 10.1073/pnas.0913900107

SI Methods

Generation of the Global dCKΔE3 KO Mice. Upon sequencing verification of targeting construct integrity, the construct was linearized and electroporated into LW-1 (129Sv/J) embryonic stem cells for integration by homologous recombination. Neomycin-resistant clones were selected (the HSV1-tk-based selection was not used) and subjected to Southern blot analysis with probes specific for exons 2 and 5 of the dCK gene to verify insertion of the targeting construct. The probes were generated by PCR using the following primers: Exon 2 probe, E2-left 5′-GAGAAAGGTCTCAGTGTTTCTGC-3′ and E2-right 5′-GGCCATGGAGACCAGACG-3′; Exon 5 probe, E5-left 5′-TCTGGCTAAAATAACTACTGATAGGG-3′ and E5-right 5′-TTGGGAAAATGAGCAAATCC-3′. Two positive clones were selected and expanded for blastocyst injection followed by implantation into a pseudopregnant female. Chimeric pups were selected and crossed with C57BL/6 mice. Agouti pups were selected and subjected to Southern blot (as described in ref. 1) and PCR genotyping to verify germline transmission of the targeted allele. For PCR-based genotyping, genomic DNA was isolated from mouse tail lysates by using the PureLink Genomic DNA kit (Invitrogen). Touchdown PCR for *dCK* alleles was performed as described in ref. 2, using the following primers: P1 5′-AACTGCTGAGCCATCTCTCC-3′, P2 5′-AAAAATAATACAGGTTTCTCTGCATC-3′, and P3 5′-GGGCTCTATGGCTTCTGAGG-3′.

Agouti mice with verified germline transmission of the targeting construct were then crossed with B6.C-Tg(CMV-cre)1Cgn/J mice (Jackson Laboratories), which express Cre recombinase in germ cells, to generate $dCK^{flox/+}$;$CMVCre^{Tg}$ mice. $dCK^{flox/+}$;$CMVCre^{Tg}$ mice were then crossed with C57BL/6 mice to obtain heterozygous knockout ($dCK^{+/-}$) mice without the Cre transgene. $dCK^{+/-}$ mice lacking the Cre transgene were identified by PCR genotyping and were subsequently intercrossed to yield the WT, Het, and global KO littermates that were used for these studies.

MicroPET/CT Imaging. Mice were kept warm, under gas anesthesia (2% isoflourane), and injected with 200 μCi of [^{18}F]FAC (i.v). A 1-h interval for uptake was allowed between probe administration and microPET/CT scanning. Data were acquired by using a Siemens Preclinical Solutions microPET Focus 220 and a MicroCAT II CT instrument. MicroPET data were acquired for 10 min and reconstructed by using statistical maximum a posteriori probability algorithms (MAP) into multiple frames (3). The spatial resolution of PET is ~1.5 mm, 0.4 mm voxel size. CT images are at low-dose 400-μm resolution acquisitions, with a 200-μm voxel size. MicroPET and microCT images were co-registered by using the method described in ref. 4. Three-dimensional regions of interest (ROI) were drawn by using AMIDE software (5). The color scale is proportional to tissue concentration with red being the highest, and lower values in yellow, green, and blue.

Antibodies and Flow Cytometry. WT and dCK KO littermates were killed at 6–8 weeks of age, and their hematopoietic and lymphoid organs were extracted and processed for flow cytometry staining. Bone marrow was flushed by using PBS, and spleens and thymi were dissociated with glass slides in DMEM media. All dissociated tissues were run through a 40-μm filter to make single cell suspensions. Splenocytes were further treated with ACK buffer (BioWhittaker) to hypotonically lyse red blood cells. CD4-PE (RM4-5), CD8α-PE-Cy7 (53-6.7), CD44-APC-Alexa750 (IM7) (eBioscience), and CD25-APC (PC61) (BD Biosciences) were used to stain thymocytes. B220-PE-Cy7 (RA3-6B2), IgM-FITC (II/41), and CD43-PE (S7) (eBioscience) were used to stain bone marrow cells for B cell Hardy fraction determination. Leukocytes from peripheral blood and dissociated lymph nodes and spleens were stained with CD3ε-APC (145-2C11), CD11b-FITC (M1/70) (eBioscience), CD19-APC-Cy7 (1D3) (BD Biosciences), and previously noted CD4 and CD8 antibodies. All staining conditions included 7-AAD (BD Biosciences) for dead cell exclusion during analysis. Splenocytes were also stained with CD45-APC (30-F11) (eBioscience) and Ter119-PE (TER-119) antibodies (BD Bioscience) and thiazole orange RNA dye (AnaSpec) to determine reticulocyte populations. Ki67 staining was performed on thymocytes by using previously noted antibodies, followed by fixation in 0.5% paraformaldehyde and permeabilization with 0.1% saponin and then incubation with Ki67-FITC (B56) (BD Biosciences). All fluorescent staining was performed according to the manufacturers' suggested methods. All data were acquired on BD Biosciences FACSCanto and LSRII flow cytometers running FACSDiva software, and all data were processed by using FlowJo analytical software (Tree Star).

1. Brown T (1993) Southern blotting. *Curr Protoc Immunol* 10.6 (Suppl 6):1–9.
2. Korbie DJ, Mattick JS (2008) Touchdown PCR for increased specificity and sensitivity in PCR amplification. *Nat Protoc* 3:1452–1456.
3. Qi J, Leahy RM, Cherry SR, Chatziioannou A, Farquhar TH (1998) High-resolution 3D Bayesian image reconstruction using the microPET small-animal scanner. *Phys Med Biol* 43:1001–1013.
4. Chow PL, Stout DB, Komisopoulou E, Chatziioannou AF (2006) A method of image registration for small animal, multi-modality imaging. *Phys Med Biol* 51:379–390.
5. Loening AM, Gambhir SS (2003) AMIDE: a free software tool for multimodality medical image analysis. *Mol Imaging* 2:131–137.

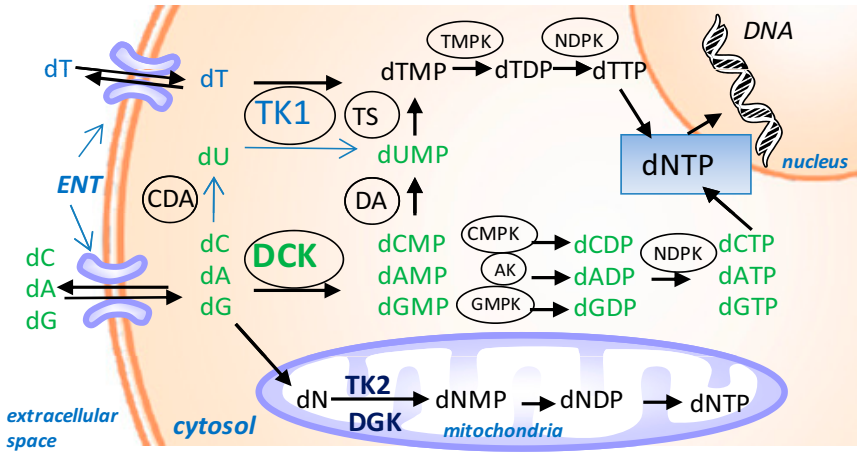

Fig. S1. dCK regulates a rate-limiting step in the nucleoside salvage pathway. dCK is the only salvage enzyme that can supply cells with all four precursors of DNA, three of them through direct phosphorylation and trapping of dC, dA, and dG, and the fourth through metabolic processing of dCMP to dTMP. ENT, equilibrative nucleoside transporter; CDA, cytidine deaminase; DA, dCMP deaminase; TS, thymidylate synthase; AK, adenylate kinase; GMPK, guanylate kinase; CMPK, cytidylate kinase; TMPK, thymidylate kinase; NDPK, nucleotide diphosphate kinase.

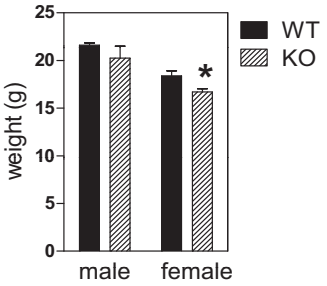

Fig. S2. Comparable developmental growth of dCK KO and WT littermates. The female KO mice weigh ~1 g less than WT counterparts at 6 weeks of age [*, $P < 0.01$; $n = 5$ (WT) and 10 (KO)].

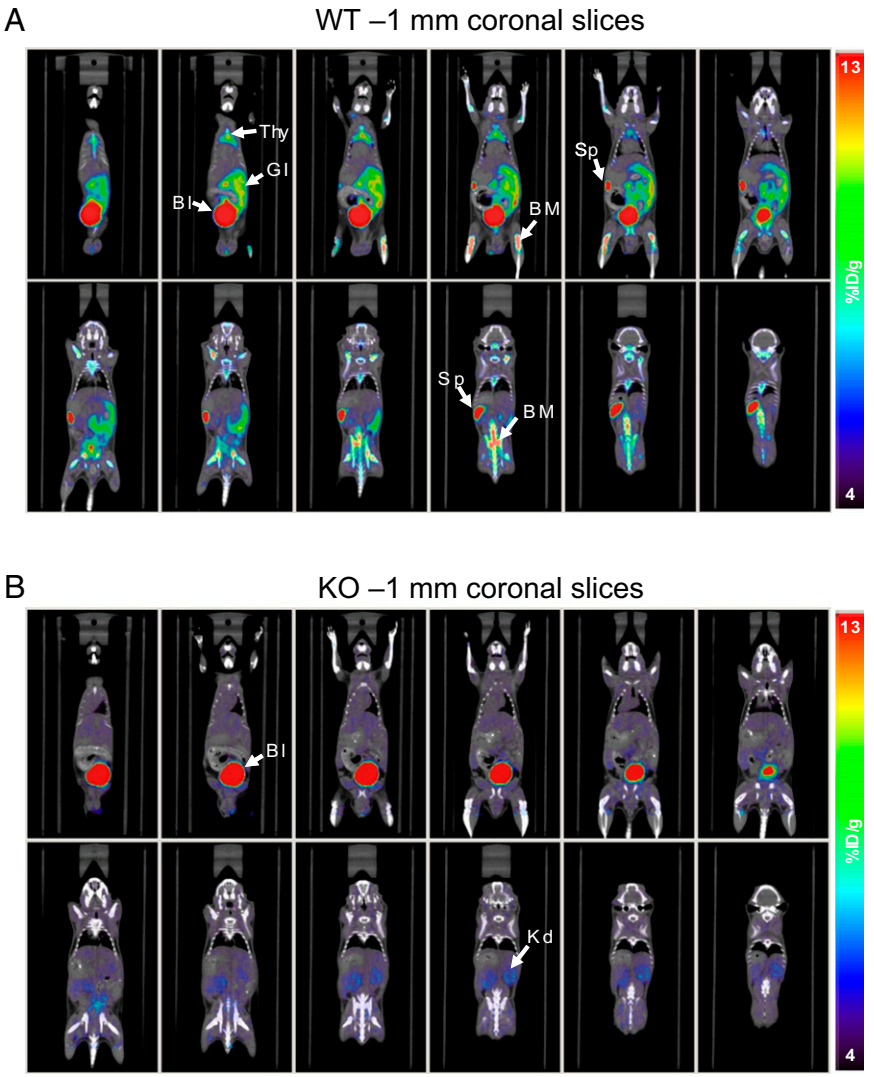

Fig. S3. Lack of in vivo uptake of [^{18}F]FAC in DCK KO mice. (*A* and *B*) One-millimeter coronal slices of WT (*A*) and DCK KO (*B*) mice imaged 60 min after i.v. administration of 200 μCi of [^{18}F]FAC. Thy, thymus; BM, bone marrow; Sp, spleen; GI, gastrointestinal tract; Kd, kidney; Bl, bladder.

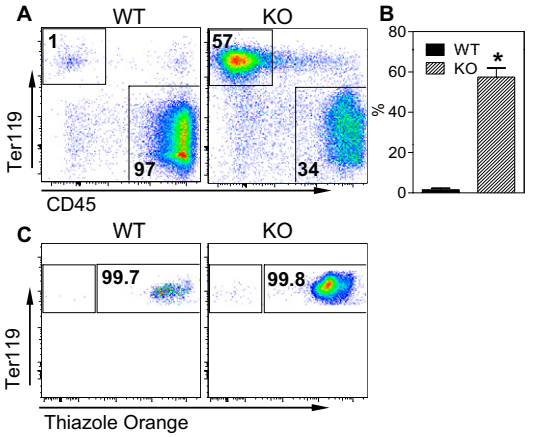

Fig. S4. Increased reticulocyte population in the dCK KO spleens. (*A*) Representative FACS plot showing the erythroid (Ter119$^+$) and myeloid/lymphoid (CD45$^+$) population. Splenocytes were analyzed after ACK buffer treatment to hypotonically lyse red blood cells. (*B*) Quantification of erythroid populations (n = 3 for each genotype). (*C*) Splenocytes were also stained with the thiazole orange RNA dye to distinguish reticulocytes from red blood cells that have resisted the hypotonic treatment.

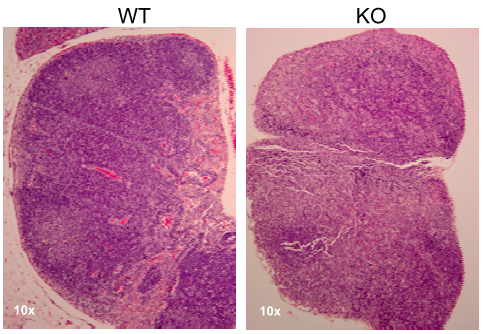

Fig. S5. Abnormal histology of dCK KO peripheral lymph nodes. Note the poor delineation between the cortex and medulla and the lack of clearly discernable follicles.

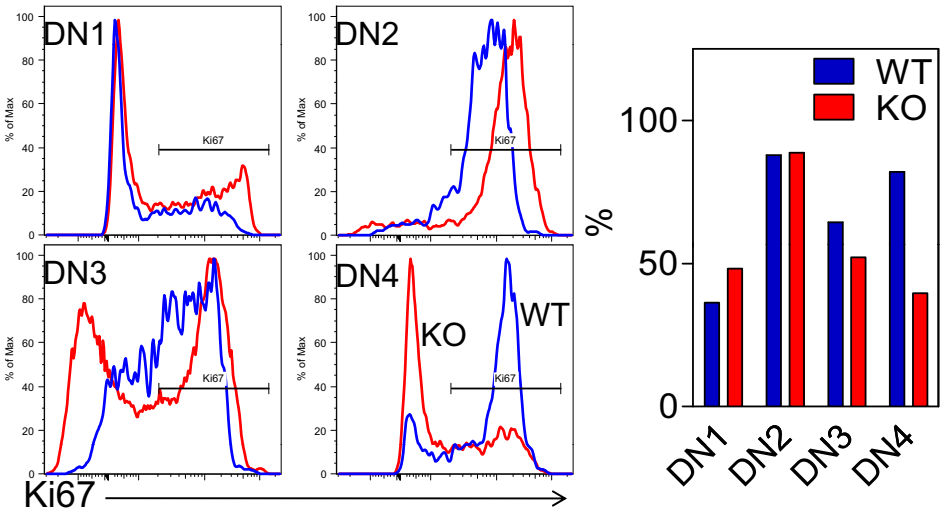

Fig. S6. Decreased expression of the Ki67 proliferation marker in dCK KO thymocytes (red traces and bars) compared to WT thymocytes (blue traces and bars) at the double negative 4 (DN4) stage of thymic development.

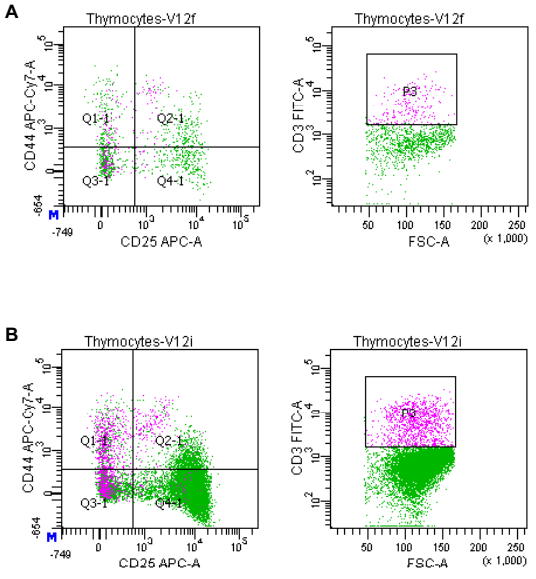

Fig. S7. TCR expression at the DN4 stage of thymic T cell development. Thymocytes were stained for CD4, CD8, CD25, and CD44 development markers and with CD3ε to determine presence of pre-TCR complexes in the DN4 stage. dCK WT (*A*) and KO (*B*) thymocytes demonstrate positive CD3ε staining (purple dots) in the DN4 stage population after TCR β chain rearrangement and surface expression in the DN3 stage. Positive CD3ε staining in the DN1-2 population most likely reflects the presence of NK cells.